

Shedding light on the pion production in heavy-ion collisions for constraining the high-density symmetry energy

Heng-Jin Liu, Hui-Gan Cheng, and Zhao-Qing Feng*

School of Physics and Optoelectronics, South China University of Technology, Guangzhou 510640, China

(Dated: April 7, 2023)

Within the framework of the quantum molecular dynamics transport model, the pion production and constraint of the high-density symmetry energy in heavy-ion collisions near threshold energy have been thoroughly investigated. The energy conservation in the decay of resonances and reabsorption of pions in nuclear medium are taken into account. The density profile of pion production, energy conservation and pion potential are analyzed by the model. The isospin diffusion in the low-density region ($0.2\rho_0 - 0.8\rho_0$) and high-density region ($1.2\rho_0 - 1.8\rho_0$) is investigated by analyzing the neutron/proton and π^-/π^+ ratios in the isotopic reactions of $^{132}\text{Sn} + ^{124}\text{Sn}$ and $^{108}\text{Sn} + ^{112}\text{Sn}$ at the incident energy of 270 MeV/nucleon, in which the symmetry energy manifests the opposite contribution. The controversial conclusion of the π^-/π^+ ratio for constraining the high-density symmetry energy by different transport models is clarified. A soft symmetry energy with the slope parameter of $L(\rho_0) = 42 \pm 25$ MeV by using the standard error analysis within the range of 1σ is obtained by analyzing the experimental data from the S π RIT collaboration.

PACS number(s): 21.65.Ef, 21.65.Jk, 24.10.Lx

Keywords: High-density symmetry energy; Neutron/proton ratio, π^-/π^+ ratio; Transverse momentum spectra; LQMD transport model

1. INTRODUCTION

Heavy-ion collisions at intermediate energies under extreme conditions, such as high density, high temperature, and high isospin asymmetry, provide a good environment for exploring the properties of dense nuclear matter. The particle production, emission mechanism and phase-space distributions bring the information of the hot and compressed nuclear matter. Pion meson has been always attracted much attention since it was predicted theoretically as a propagator of the strong interaction [1] and later discovered by observing the cosmic rays in experiments [2]. Nowadays, pions might be created in laboratories via different reactions, such as heavy-ion collisions, photon, lepton and hadron induced reactions, electron-positron colliding etc. Particles produced in the GeV energy range manifest the information of the high-density nuclear matter and might be modified by the nuclear medium [3]. The nuclear equation of state (EOS) is expressed with the energy per nucleon as $E(\rho, \delta) = E(\rho, \delta = 0) + E_{\text{sym}}(\rho)\delta^2 + \mathcal{O}(\delta^4)$ in terms of baryon density $\rho = \rho_n + \rho_p$ and relative neutron excess $\delta = (\rho_n - \rho_p)/(\rho_n + \rho_p)$, where $E_{\text{sym}}(\rho)$ is the symmetry energy [4–6]. The symmetry energy at the subsaturation density has important application in understanding the structure of weakly bound nuclei, nucleon-nucleon correlation, pasta structure of neutron star etc, which was extensively investigated by different approaches, such as the Pygmy dipole resonance, heavy-ion collision, fast fission, electron-nucleus scattering etc [7–16]. The high-density symmetry energy is related to the issues of compact stars, such as the phase transition, binary neutron star merging, tidal deformation etc [17–22], which is still not well understood up to now. To extracting the den-

sity dependence of symmetry energy, new experiments are being carried out at the facility in the world, such as Radioactive Isotope Beam Facility (RIBF) in Japan [23], Rare Isotope Science Project in Korea (RAON) [24], Facility for Rare Isotope Beams (FRIB) in the USA [25], the Cooling Storage Ring (CSR) and the High Intensity Accelerator Facility (HIAF) in China [26].

Pions produced in heavy-ion collisions carry the high-density information of nuclear matter and the π^-/π^+ ratio might be a probe of high-density symmetry energy [27]. There has been collected a number of experimental data for the pion production in heavy-ion collisions, such as the BEVALAC with the Berkeley Streamer Chamber [28, 29], the DIOGENE at the Saturne synchrotron in Saclay [30], the FOPI collaboration at the beam energies from 0.4A to 1.5A GeV [31], the S π RIT collaboration for the systems $^{132}\text{Sn} + ^{124}\text{Sn}$ and $^{108}\text{Sn} + ^{112}\text{Sn}$ at 270A MeV [32]. The opposite conclusion for constraining the high-density symmetry energy was obtained by analyzing the FOPI data of the π^-/π^+ excitation function with the different transport models [33, 34], namely the ‘pion puzzle’. At the near threshold energy, the pion mesons are mainly produced via the decay of $\Delta(1232)$ resonance. The pion dynamics is modified in the nuclear environment, i.e., the pion-nucleon potential, elementary production cross section, threshold energy, decay width of resonance, reabsorption process via the reaction $\pi N \leftrightarrow \Delta$ etc. The influence of the π potential on the pion dynamics in heavy-ion collisions has been investigated via transport models [35–42]. Recently, the uncertainties in transport models for heavy-ion collisions are investigated by the transport model evaluation project (TMEP) [43, 44]. More sophisticated investigation of the pion-nucleon potential is still necessary, in particular, distinguishing the

isospin effect, manifesting the momentum and density dependence and reproducing the pion-nucleus scattering data. Both the pion potential and stiffness of symmetry energy influence the π^-/π^+ momentum spectra in heavy-ion collisions.

In this work, the pion dynamics and high-density symmetry energy is investigated with the Lanzhou Quantum Molecular Dynamics (LQMD) transport model. The article is organized as follows. In Sec. 2, we briefly introduce the theoretical approach. The calculated results and comparison with the FOPI and S π RIT data are shown in Sec. 3. A summary is given in Sec. 4.

2. BRIEF DESCRIPTION OF THE LQMD TRANSPORT MODEL

In the LQMD transport model, the production of resonances, hyperons and mesons is coupled in the reactions of meson-baryon and baryon-baryon collisions, which has been used for the nuclear dynamics in heavy-ion collisions and hadron induced reactions [14, 45]. The temporal evolutions of nucleons and nucleonic resonances are described by Hamilton's equations of motion under the self-consistently generated two-body and three-body potentials with the Skyrme effective interaction. The symmetry energy is composed of three parts, namely, the kinetic energy from Fermi motion, the local density-dependent interaction, and the momentum-dependent potential, which reads as

$$E_{sym}(\rho) = \frac{1}{3} \frac{\hbar^2}{2m} \left(\frac{3}{2} \pi^2 \rho \right)^{2/3} + E_{sym}^{loc}(\rho) + E_{sym}^{mom}(\rho). \quad (1)$$

The stiffness of symmetry energy is adjusted by

$$E_{sym}^{loc}(\rho) = \frac{1}{2} C_{sym} (\rho/\rho_0)^{\gamma_s}. \quad (2)$$

The parameter C_{sym} is 52.5 MeV, and the stiffness parameter γ_s is adjusted for getting the density dependence of symmetry energy, e.g., the values of 0.3, 1, and 2 being the soft, linear, and hard symmetry energy, corresponding to the slope parameters $[L(\rho_0) = 3\rho_0 dE_{sym}(\rho)/d\rho|_{\rho=\rho_0}]$ of 42, 82, and 139 MeV, respectively. As shown in Fig. 1(a), it can be seen that in all cases of symmetry energy at the saturation density ($\rho_0 = 0.16 \text{ fm}^{-3}$) with the value of 31.5 MeV. The different slope of symmetry energy influences the neutron/proton ratio and also the mass-radius relation of neutron star. The hard symmetry energy ($L=139 \text{ MeV}$) results in the more repulsive force of neutron-neutron interaction in the neutron-rich matter and consequently the lower neutron/proton ratio in the high-density domain. The symmetry energy dominates the isospin diffusion in heavy-ion collisions and leads to the isospin density difference. The larger neutron/proton ratio in the density region of $1.2 \leq \rho/\rho_0 \leq 1.8$ with the soft symmetry energy

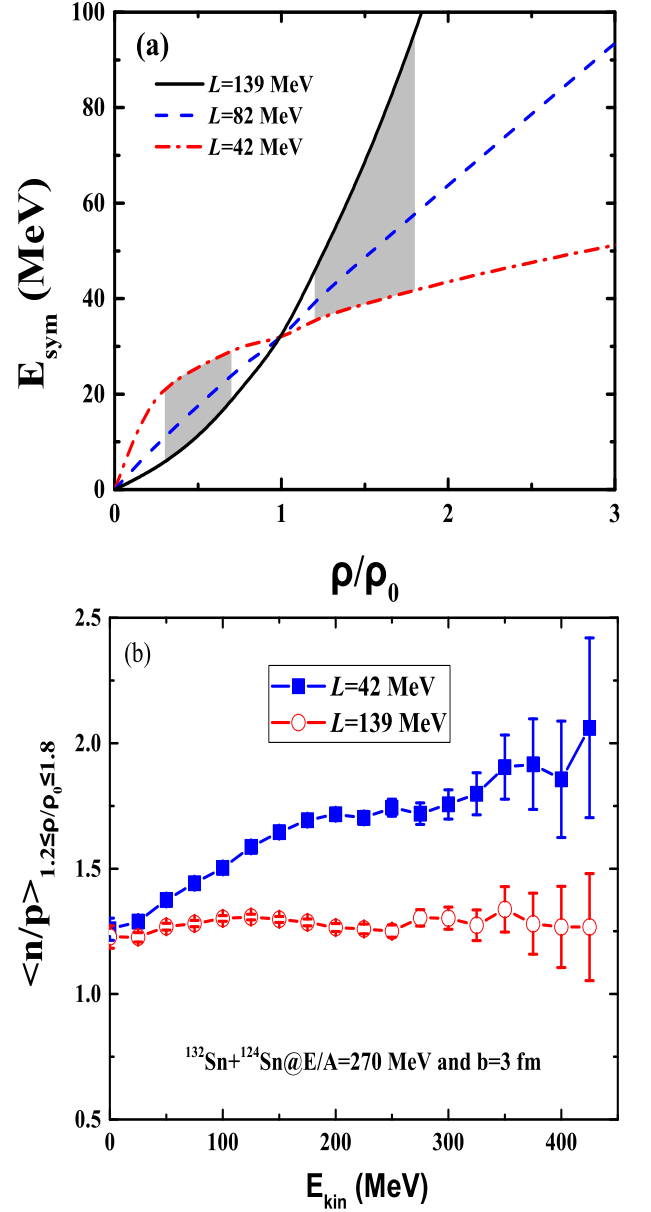


FIG. 1. (a) The density dependence of nuclear symmetry energy with different stiffness and (b) the neutron/proton ratio in the density region of $1.2 \leq \rho/\rho_0 \leq 1.8$ with the dense matter formed in collisions of $^{132}\text{Sn}+^{124}\text{Sn}$ at the beam energy of 270 MeV/nucleon and with the impact parameter of $b=3 \text{ fm}$.

in the temporal evolution of $^{132}\text{Sn}+^{124}\text{Sn}$ is obtained as shown in Fig. 1(b), in particular in the regime of kinetic energy above 100 MeV. The stiffness of symmetry energy might be constrained by the isospin observables in heavy-ion collisions.

The transportation of pion in nuclear medium is also governed by Hamiltonian as

$$H_M = \sum_{i=1}^{N_M} [V_i^{Coul} + \omega(\mathbf{p}_i, \rho_i)]. \quad (3)$$

The Coulomb interaction is given by

$$V_i^{Coul} = \sum_{j=1}^{N_B} \frac{e_i e_j}{r_{ij}} \quad (4)$$

with $r_{ij} = |\mathbf{r}_i - \mathbf{r}_j|$. Here the N_M and N_B are the total numbers of mesons and baryons including charged resonances, respectively. It should be noted that the pion meson is taken as the point particle and the Coulomb interaction between mesons is neglected owing to the limited numbers in comparison with the baryons.

The pion energy in the nuclear medium is composed of the isoscalar and isovector contributions as

$$\omega_\pi(\mathbf{p}_i, \rho_i) = \omega_{isoscalar}(\mathbf{p}_i, \rho_i) + C_\pi \tau_z \delta(\rho/\rho_0)^{\gamma_\pi}. \quad (5)$$

Here the isovector coefficient $C_\pi = \rho_0 \hbar^3 / (4f_\pi^2) = 36$ MeV, isospin asymmetry $\delta = (\rho_n - \rho_p) / (\rho_n + \rho_p)$ and isospin splitting parameter $\gamma_\pi = 2$. The isospin quantities are set to be $\tau_z = -1, 0$, and 1 for π^+ , π^0 , and π^- , respectively [39]. The isoscalar part $\omega_{isoscalar}$ is estimated by the Δ -hole model [46, 47].

The energy balance in the decay of resonances and re-absorption of pion in nuclear medium is satisfied by the relation as

$$\sqrt{m_R^2 + \mathbf{p}_R^2} + U_R(\rho, \delta, \mathbf{p}) = \sqrt{m_N^2 + (\mathbf{p}_R - \mathbf{p}_\pi)^2} + U_N(\rho, \delta, \mathbf{p}) + \omega_\pi(\mathbf{p}_\pi, \rho) + V_{\pi N}^{Coul}. \quad (6)$$

The \mathbf{p}_R and \mathbf{p}_π are the momenta of resonance and pion, respectively. The term $V_{\pi N}^{Coul}$ has the contribution only for the charged pair channels of $\Delta^0 \leftrightarrow \pi^- + p$ and $\Delta^{++} \leftrightarrow \pi^+ + p$. The optical potential can be evaluated from the in-medium energy $V_\pi^{opt} = \omega_\pi(\mathbf{p}, \rho) - (m_\pi^2 + \mathbf{p}^2)^{1/2}$. The U_R and U_N are the single-particle potentials for resonance and nucleon. For example, the $\Delta(1232)$ optical potential is calculated via the nucleon optical potential by

$$\begin{aligned} U_{\Delta^-} &= U_n, & U_{\Delta^{++}} &= U_p, & U_{\Delta^+} &= \frac{1}{3}U_n + \frac{2}{3}U_p, \\ U_{\Delta^0} &= \frac{1}{3}U_p + \frac{2}{3}U_n, \end{aligned} \quad (7)$$

where the U_n and U_p are the single-particle potentials for neutron and proton, respectively. The N^* -nucleon potential is taken as the same with the nucleon-nucleon potential. The density, isospin and momentum dependent single-nucleon potential is obtained as follows

$$\begin{aligned} U_\tau(\rho, \delta, \mathbf{p}) &= \alpha \left(\frac{\rho}{\rho_0} \right) + \beta \left(\frac{\rho}{\rho_0} \right)^\gamma + E_{sym}^{loc}(\rho) \delta^2 \\ &+ \frac{\partial E_{sym}^{loc}(\rho)}{\partial \rho} \rho \delta^2 + E_{sym}^{loc}(\rho) \rho \frac{\partial \delta^2}{\partial \rho_\tau} \\ &+ \frac{1}{\rho_0} C_{\tau, \tau} \int d\mathbf{p}' f_\tau(\mathbf{r}, \mathbf{p}) [\ln(\epsilon(\mathbf{p} - \mathbf{p}')^2 + 1)]^2 \\ &+ \frac{1}{\rho_0} C_{\tau, \tau'} \int d\mathbf{p}' f_{\tau'}(\mathbf{r}, \mathbf{p}) \\ &\times [\ln(\epsilon(\mathbf{p} - \mathbf{p}')^2 + 1)]^2. \end{aligned} \quad (8)$$

Here $\tau \neq \tau'$, $\partial \delta^2 / \partial \rho_n = 4\delta \rho_p / \rho^2$ and $\partial \delta^2 / \partial \rho_p = -4\delta \rho_n / \rho^2$. The nucleon effective (Landau) mass in nuclear matter of isospin asymmetry $\delta = (\rho_n - \rho_p) / (\rho_n + \rho_p)$ with ρ_n and ρ_p being the neutron and proton density, respectively, is calculated through the potential as $m_\tau^* = m_\tau / \left(1 + \frac{m_\tau}{|\mathbf{p}|} \left| \frac{dU_\tau}{d\mathbf{p}} \right| \right)$ with the free mass m_τ at Fermi momentum $\mathbf{p} = \mathbf{p}_F$. The parameters α , β , γ and ρ_0 are set to be the values of -215.7 MeV, 142.4 MeV, 1.322 and 0.16 fm^{-3} , respectively. The $C_{\tau, \tau} = C_{mom}(1+x)$, $C_{\tau, \tau'} = C_{mom}(1-x)$ ($\tau \neq \tau'$) and the isospin symbols $\tau(\tau')$ represent proton or neutron. The values of 1.76 MeV, $500 \text{ c}^2/\text{GeV}^2$ are taken for the C_{mom} and ϵ , respectively, which result in the effective mass $m^*/m=0.75$ in nuclear medium at saturation density for symmetric nuclear matter. The parameter x as the strength of the isospin splitting with the value of -0.65 is taken in this work, which has the mass splitting of $m_n^* > m_p^*$ in nuclear medium. A compression modulus of $K=230$ MeV for isospin symmetric nuclear matter is obtained at the saturation density. Recently, the influence of the pion potential on pion dynamics in heavy-ion collisions has been extensively investigated with different transport models [38–41, 48–50].

3. RESULTS AND DISCUSSION

The isospin diffusion in heavy-ion collisions is associated with the gradient of isospin density $\rho_n - \rho_p$, in which the symmetry energy plays a significant role on the rearrangement of nucleons in phase space. The neutron and proton density distributions vary with the evolution of reaction system and neutron/proton ratio is diverse in the different density range. To extract the high-density symmetry energy, the observables emitted from the high-density domain in nuclear collisions are expected. The neutron/proton ratio is a direct probe for extracting the high-density symmetry energy. But detecting the neutrons with high statistics in experiments is still a difficulty task. We calculated the kinetic energy spectra of neutron/proton (N/Z) ratio of free nucleons produced in collisions of $^{132}\text{Sn} + ^{124}\text{Sn}$ and $^{108}\text{Sn} + ^{112}\text{Sn}$ at 270 A MeV with different symmetry energy as shown in Fig. 2. It is obvious that the hard symmetry energy with $L=139$ MeV leads to the larger N/Z ratio, in particular at the energies above 100 MeV for the neutron-rich system. The results are consistent with the conclusion in Fig. 1 (b), which is caused from the more repulsive interaction for neutrons in the dense neutron-rich matter. More free neutrons are created with the hard symmetry energy. Hunting the measurable quantities for constraining the high-density symmetry energy is very necessary, e.g., π^-/π^+ , K^0/K^+ , Σ^-/Σ^+ etc.

The symmetry energy as a major ingredient in the nuclear equation of state plays a significant role on

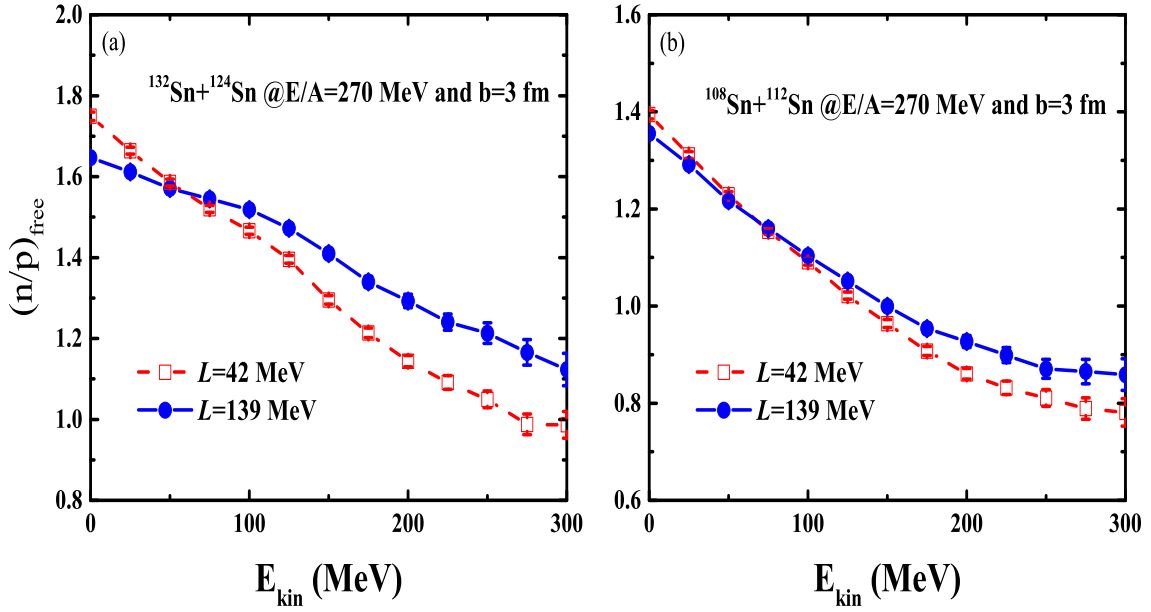


FIG. 2. The kinetic energy spectra of free neutron/proton ratio produced in collisions of $^{132}\text{Sn}+^{124}\text{Sn}$ (left panel) and $^{108}\text{Sn}+^{112}\text{Sn}$ (right panel), respectively.

the mass-radius relation and maximal mass of neutron stars, phase transition from quark-gluon plasma to hadron phase, nuclear structure of rare isotopes etc. The high-density behavior of symmetry energy from the pion production in heavy-ion collisions has been extensively investigated via transport models, such as the isospin dependent Boltzmann-Uehling-Uhlenbeck (IBUU) and relativistic Vlasov-Uehling-Uhlenbeck (RVUU) [49, 51–53]. Recently, the transverse momentum spectra of pions has been measured by the S π RIT collaboration [32, 54]. In comparison with the previous works, the energy conservation is considered in the decay of resonances. The systematic density profile of pion production in collisions of $^{132}\text{Sn} + ^{124}\text{Sn}$ at 270A MeV is shown as in Fig. 3. The black line denotes the total pion production ($\pi^- + \pi^0 + \pi^+$). And the red dashed and the blue dotted-dashed lines represent π^- and π^+ , respectively. The pion is counted once it is created in the whole temporal evolution. It is obvious that a number of pions are produced in the low-density region, but pions at the suprasaturation densities are still appreciable. The low-density pions is mainly caused from the rescattering processes, i.e., $\pi N \leftrightarrow \Delta(1232)$ and $\Delta(1232)N \leftrightarrow NN$ [50]. Therefore, to extract the high-density information of symmetry energy, one needs to distinguish the final pions from the different density range. It is known that the π^-/π^+ ratio of primordial pions without the rescatterings is approximately satisfied to the quadratic relation $\pi^-/\pi^+ = \frac{5n^2+np}{5p^2+np} \approx (n/p)^2$ [46]. To clarify the pion production in the different density range, shown in Fig. 4 is the kinetic energy spectra of π^-/π^+ ratio in the density region of $0.2 \leq \rho/\rho_0 \leq 0.8$ and $1.2 \leq \rho/\rho_0 \leq 1.8$,

respectively. It is pronounced that the symmetry energy effect is opposite in the different density domain, namely, the larger π^-/π^+ ratio with the hard symmetry energy in the low-density region, but the lower π^-/π^+ value at high densities. Moreover, the average π^-/π^+ ratio in the low-density region of $0.2 \leq \rho/\rho_0 \leq 0.8$ is close to the square of N/Z ratio (2.43) of reaction system. But the π^-/π^+ ratio in the high-density region is approximately the average N/Z value (1.56) at the kinetic energies below 100 MeV. Therefore, the π^-/π^+ ratio from the total pion multiplicities is indistinguishable for extracting the high-density symmetry energy. The density profile of pions is influenced by the rescattering cross sections and pion evolution in nuclear medium, which might be different in transport models although the total multiplicity is similar. The phase-space distribution of pion is associated with its emission local density. The kinetic energy or transverse momentum spectra of π^-/π^+ ratio might be available probes for constraining the high-density symmetry energy.

The phase-space distribution of emitted particles in heavy-ion collisions manifest the in-medium properties, i.e., the rapidity, transverse momentum, kinetic energy, invariant mass spectra etc. More information of the pion production can be obtained from the transverse momentum spectra. Shown in Fig. 5 is a comparison of energy conservation in the decay of resonance and pion optical potential on the pion production in collisions of $^{132}\text{Sn}+^{124}\text{Sn}$ and $^{108}\text{Sn}+^{112}\text{Sn}$ at the incident energy of 270A MeV with the soft symmetry energy. Inclusion of the energy conservation enhances the high-momentum pion production for both systems. The pion-nucleon po-

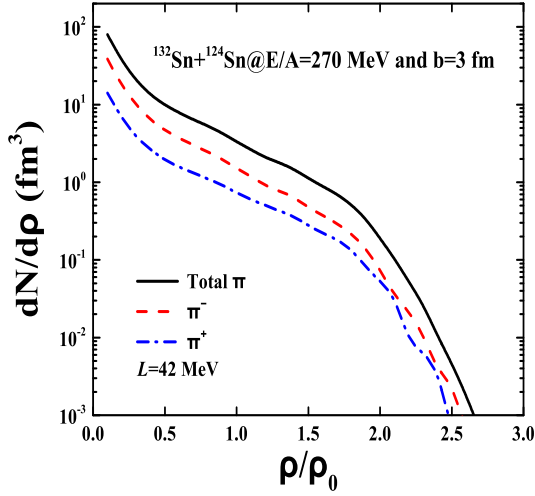


FIG. 3. The density profile of pion production in collisions of $^{132}\text{Sn}+^{124}\text{Sn}$ at 270A MeV.

tential leads to the reduction of pion yields because of the attractive interaction, in particular for the π^+ production. The experimental data of transverse momentum spectra from the S π RIT collaboration [32] are nicely reproduced with the inclusion of energy conservation relation and pion potential. The symmetry energy effect is also analyzed as shown in Fig. 6. The effect is pronounced for the π^- production and the soft symmetry energy enhances the yields. The π^+ spectra weakly depend on the stiffness of symmetry energy because the proton-proton and proton-neutron collisions are almost not influenced by the symmetry energy in neutron-rich system. It is concluded that π^-/π^+ ratio is also enhanced with the symmetry energy of $L=42$ MeV and consistent with the high-density results in Fig. 4(b). The high-transverse momentum pions are mainly produced from the high-density zone in nuclear collisions and might be probes of high-density symmetry energy.

To eliminate the Coulomb interaction and reduce some uncertainties, we analyzed the double ratios (DRs) in the isotopic reactions, which are defined as the relation $\text{DR}(n/p) = (n/p)_{^{132}\text{Sn}+^{124}\text{Sn}}^{\text{free}} / (n/p)_{^{108}\text{Sn}+^{112}\text{Sn}}^{\text{free}}$ and $\text{DR}(\pi^-/\pi^+) = (\pi^-/\pi^+)_{^{132}\text{Sn}+^{124}\text{Sn}} / (\pi^-/\pi^+)_{^{108}\text{Sn}+^{112}\text{Sn}}$, respectively. The method has been used for constraining the symmetry energy at the subsaturation density and the isospin splitting of nucleon effective mass in nuclear matter [55]. The symmetry energy effect is pronounced at the high kinetic energies (high transverse momenta) in the isotopic reactions as shown in Fig. 7, i.e., in the domain of $E_{\text{kin}} > 100$ MeV or $p_T > 150$ MeV/c. The double ratio of neutron/proton has more obvious symmetry energy effect in comparison with the case of π^-/π^+ , but the larger DR value for the pion production. The complementary observables manifest that the DRs of high kinetic energy or transverse momentum might be probes for extracting the high-density symmetry

energy. The slope parameter of symmetry energy at saturation density $L(\rho_0) = 42 \pm 25$ is obtained by using the standard error analysis method within the range 1σ . Due to the mixing of pions produced at high and low densities, the symmetry energy effect on DR is n. However, at high transverse momentum ($p_T \geq 150$ MeV/c) the DR exhibits significant sensitivity to the symmetry energy, and the effect is about 20%. It is noted that the constraint of $42 \text{ MeV} < L < 117 \text{ MeV}$ is obtained by the dcQMD calculations. Different with the dcQMD model, we fixed the isospin splitting of nucleon effective mass, i.e., $(m_n^* - m_p^*)/m_n = 0.04$ with the isospin asymmetry of $\delta = 0.2$ at the saturation density.

4. CONCLUSIONS

In summary, the isospin diffusion in the isotopic reactions of $^{132}\text{Sn} + ^{124}\text{Sn}$ and $^{108}\text{Sn} + ^{112}\text{Sn}$ at the incident energy of 270 MeV/nucleon is thoroughly investigated within the LQMD transport model. The symmetry energy manifests the opposite contribution on the N/Z and π^-/π^+ ratios in the low-density region and in the high-density domain. The hard symmetry energy enhances the N/Z ratio of free nucleons, but leads to the reduction of N/Z and π^-/π^+ ratios in the high-density region. The production of pions in heavy-ion collisions spreads the whole density range and most of pions are created in the dilute nuclear matter because of the rescattering processes of pions and resonances with nucleons. The stiffness of symmetry energy is sensitive to the π^- transverse spectra, but weakly impact the π^+ production. The pion optimal potential is obvious in the high-momentum regime and influences both the π^- and π^+ spectra. Systematics analysis with the symmetry energy and pion-nucleon potential manifests the soft symmetry energy with the slope parameter $L(\rho_0) = 42 \pm 25$ MeV or stiffness parameter $\gamma_s = 0.3$ with the S π RIT data.

Acknowledgements This work was supported by the National Natural Science Foundation of China (Projects No. 12175072 and No. 11722546) and the Talent Program of South China University of Technology (Projects No. 20210115).

* Corresponding author: fengzhq@scut.edu.cn

- [1] H. Yukawa, Proceedings of the Physico-Mathematical Society of Japan **17**, 48 (1935).
- [2] C. M. G. Lattes, H. Muirhead, G. P. S. Occhialini, and C. F. Powell, Nature **159**, 694 (1947).
- [3] J. C. Kintner *et al.*, Phys. Rev. Lett. **78**, 4165 (1997).
- [4] I. Bombaci and U. Lombardo, Phys. Rev. C **44**, 1892 (1991).
- [5] V. Baran, M. Colonna, V. Greco, and M. Di Toro, Phys. Rep. **410**, 335 (2005).

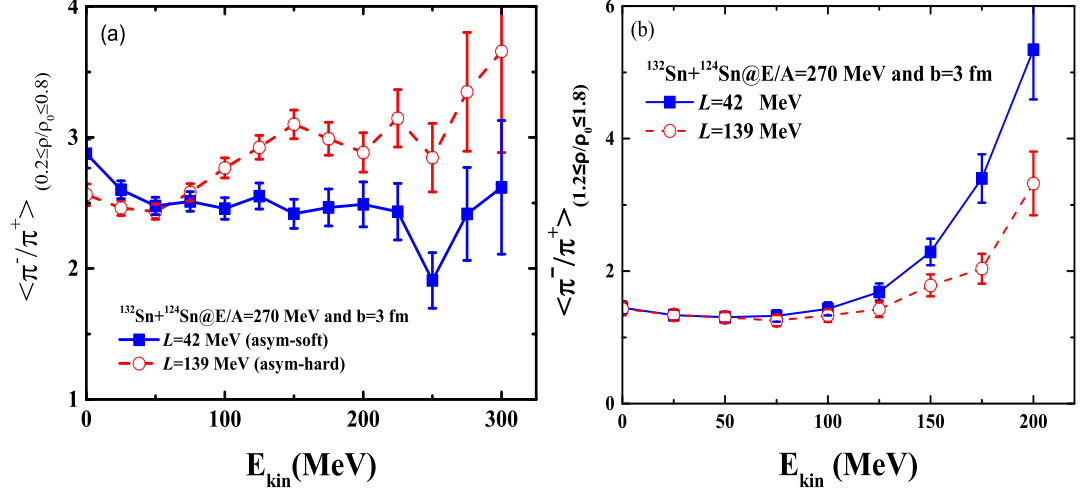


FIG. 4. The kinetic energy spectra of π^-/π^+ ratio in collisions of $^{132}\text{Sn} + ^{124}\text{Sn}$ at 270A MeV within the baryon density region for the pion production of (a) $0.2 \leq \rho/\rho_0 \leq 0.8$ and (b) $1.2 \leq \rho/\rho_0 \leq 1.8$, respectively.

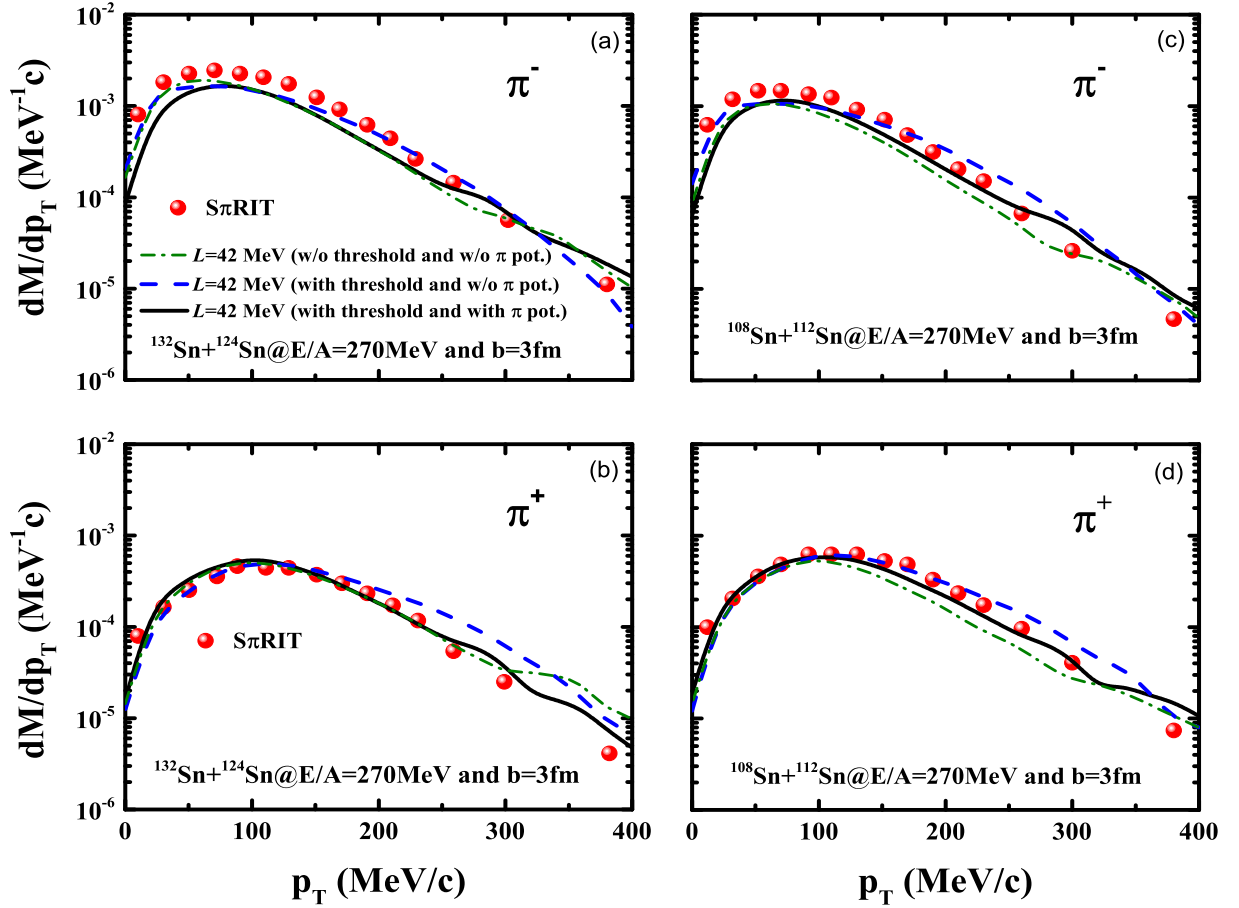


FIG. 5. Comparison of the transverse momentum spectra with the inclusion of threshold energy correction and pion potential in collisions of $^{132}\text{Sn} + ^{124}\text{Sn}$ (left panel) and $^{108}\text{Sn} + ^{112}\text{Sn}$ (right panel), respectively. The experimental data are taken from the S π RIT collaboration [32].

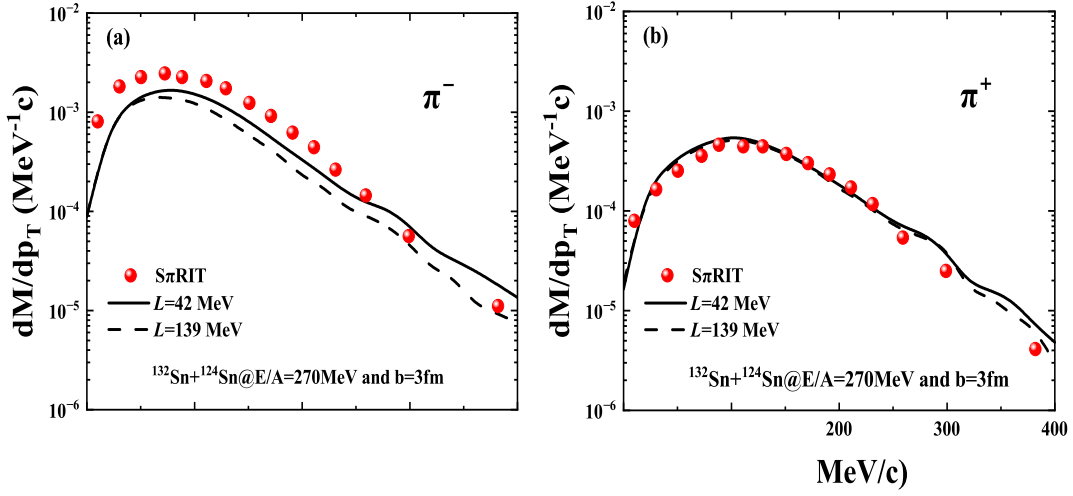


FIG. 6.
SπRIT d:

netry energy and compared with the

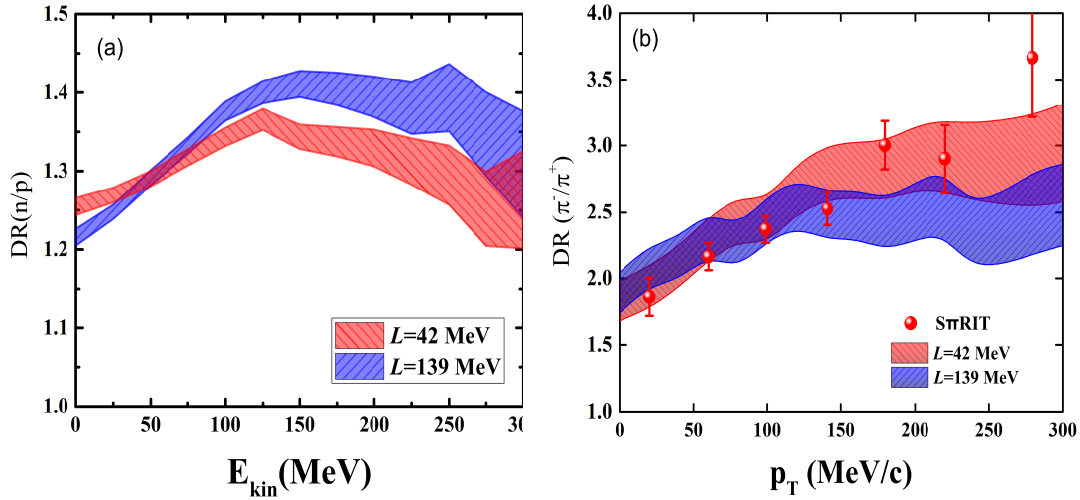


FIG. 7. The double ratios of (a) neutron/proton and (b) π^-/π^+ in the isotropic reactions of $^{132}\text{Sn} + ^{124}\text{Sn}$ and $^{108}\text{Sn} + ^{112}\text{Sn}$ at 270A MeV and $b=3$ fm. The experimental data for the pion production are taken from the SπRIT collaboration [32].

- [6] B. A. Li, L. W. Chen, and C. M. Ko, Phys. Rep. **464**, 113 (2008).
- [7] B. A. Li, C. M. Ko, and Z. Ren, Phys. Rev. Lett. **78**, 1644 (1997); B. A. Li, Phys. Rev. Lett. **85**, 4221 (2000).
- [8] L. W. Chen, C. M. Ko, B. A. Li, Phys. Rev. Lett. **94**, 032701 (2005).
- [9] N. Tsoneva and H. Lenske, Phys. Rev. C **77**, 024321 (2008).
- [10] L. G. Cao, X. Roca-Maza, G. Colò, and H. Sagawa, Phys. Rev. C **92**, 034308 (2015).
- [11] Z. Y. Sun, M. B. Tsang, W. G. Lynch *et al.*, Phys. Rev. C **82**, 051603(R) (2010).
- [12] E. De Filippo, A. Pagano, Eur. Phys. J. A **50**, 32 (2014); P. Russotto *et al.*, Phys. Rev. C **91**, 014610 (2015).
- [13] Z. Q. Feng, Phys. Rev. C **94**, 014609 (2016).
- [14] Z. Q. Feng, Nucl. Sci. Tech., **29**, 40 (2018).
- [15] Y. Zhang *et al.*, Phys. Rev. C **95**, 041602 (2017).
- [16] D. Adhikari *et al.*, (PREX Collaboration), Phys. Rev. Lett. **126**, 172502 (2021).
- [17] A. W. Steiner, M. Prakash, J. M. Lattimer, and P. J. Ellis, Phys. Rep. **411**, 325 (2015).
- [18] E. Friedman, and A. Gal, Phys. Rep. **452**, 89 (2007).
- [19] M. Di Toro, B. Liu, V. Greco, V. Baran, M. Colonna, and S. Plumari, Phys. Rev. C **83**, 014911 (2011).
- [20] A. Bauswein, S. Goriely, and H. T. Janka, Astrophys. J **773**, 78 (2013).
- [21] M. Oertel, M. Hempel, T. Klähn, and S. Typel, Rev. Mod. Phys. **89**, 015007 (2017).
- [22] S. Huth *et al.*, Nature **606**, 276 (2022).
- [23] H. Sakurai, Front. Phys. **13**, 132111 (2018).
- [24] K. Tshoo, Y. K. Kim, Y. K. Kwon *et al.*, Nucl. Instrum. Methods B **317**, 242 (2013).
- [25] P. N. Ostroumov, S. Cogan, K. Fukushima, S. Lidia, T. Maruta, A. S. Plastun, J. Wei, J. Wong, T. Yoshimoto, and Q. Zhao, Phys. Rev. Accel. Beams **22**, 040101 (2019).
- [26] J. C. Yang, J. W. Xia, G. Q. Xiao *et al.*, Nucl. Instrum. Methods B **317**, 263 (2013).
- [27] B. A. Li, Phys. Rev. Lett. **88**, 192701 (2002).

- [28] J. W. Harris *et al.*, Phys. Lett. B **153**, 377 (1985).
- [29] J. W. Harris *et al.*, Phys. Rev. Lett. **58**, 463 (1987).
- [30] J. P. Alard *et al.*, Nucl. Instrum. Methods A **261**, 379 (1987).
- [31] W. Reisdorf *et al.*, Nucl. Phys. A **781**, 459 (2007).
- [32] J. Estee *et al.*, Phys. Rev. Lett. **126**, 162701 (2021).
- [33] Z. Xiao, B. A. Li, L. W. Chen, G. C. Yong, and M. Zhang, Phys. Rev. Lett. **102**, 062502 (2009).
- [34] Z. Q. Feng and G. M. Jin, Phys. Lett. B **683**, 140 (2010).
- [35] L. Xiong, C. M. Ko, and V. Koch, Phys. Rev. C **47**, 788 (1993).
- [36] C. Fuchs, L. Sehn, E. Lehmann, J. Zipprich, and A. Faessler, Phys. Rev. C **55**, 411 (1997).
- [37] Z. Q. Feng, and G. M. Jin, Phys. Rev. C **82**, 044615 (2010).
- [38] J. Hong, and P. Danielewicz, Phys. Rev. C **90**, 024605 (2014).
- [39] Z. Q. Feng, W. J. Xie, P. H. Chen, J. Chen, and G. M. Jin, Phys. Rev. C **92**, 044604 (2015).
- [40] W. M. Guo, G. C. Yong, H. Liu, and W. Zuo, Phys. Rev. C **91**, 054616 (2015).
- [41] T. Song and C. M. Ko, Phys. Rev. C **91**, 014901 (2015).
- [42] M. D. Cozma, Phys. Rev. C **95**, 014601 (2017).
- [43] Akira Ono *et al.*, Phys. Rev. C **100**, 044617 (2019).
- [44] Hermann Wolter *et al.*, Prog. Part. Nucl. Phys. **125**, 103962 (2022).
- [45] Z. Q. Feng, Phys. Rev. C **84**, 024610 (2011); Phys. Rev. C **85**, 014604 (2012).
- [46] G. E. Brown and W. Weise, Phys. Rep. **22**, 279 (1975).
- [47] B. Friemann, V. P. Pandharipande, and Q. N. Usmani, Nucl. Phys. A **372**, 483 (1981).
- [48] M. D. Cozma, Phys Lett B **753**, 166 (2016).
- [49] Z. Zhang and C. M. Ko, Phys. Rev. C **95**, 064604 (2017).
- [50] Z. Q. Feng, Eur. Phys. J. A **53**, 30 (2017).
- [51] G. Ferini, T. Gaitanos, M. Colonna, M. Di Toro, and H. Wolter, Phys. Rev. Lett. **97**, 202301 (2006).
- [52] G. C. Yong, Phys. Rev. C **104**, 014613 (2021).
- [53] Y. Gao, G. C. Yong, Y. J. Wang, Q. F. Li, and W. Zuo, Phys. Rev. C **88**, 057601 (2013).
- [54] G. Jhang *et al.*, Phys. Lett. B **813**, 136016 (2021).
- [55] Y. F. Guo, P. H. Chen, F. Niu *et al.*, Chin. Phys. C **41**, 104104 (2017).